Atmospheric Environment 180 (2018) 206–215

Contents lists available at ScienceDirect

Atmospheric Environment

journal homepage: www.elsevier.com/locate/atmosenv

Molecular structure impacts on secondary organic aerosol formation from glycol ethers

Lijie Li[a,b], David R. Cocker III[a,b,*]

[a] University of California, Riverside, Department of Chemical and Environmental Engineering, Riverside, CA 92507, USA
[b] College of Engineering-Center for Environmental Research and Technology (CE-CERT), Riverside, CA 92507, USA

GRAPHICAL ABSTRACT

General mechanism of ether photooxidation with and without –OH functional group in ethers.

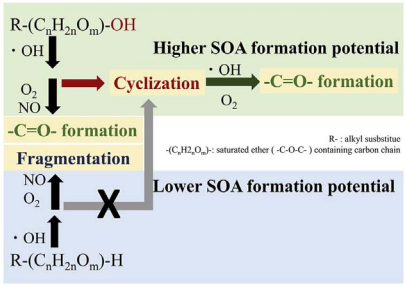

ARTICLE INFO

Keywords:
Glycol ether
Molecular structure
Consumer products
Photooxidation
Secondary organic aerosol
NO_X
HR-ToF-AMS

ABSTRACT

Glycol ethers, a class of widely used solvents in consumer products, are often considered exempt as volatile organic compounds based on their vapor pressure or boiling points by regulatory agencies. However, recent studies found that glycol ethers volatilize at ambient conditions nearly as rapidly as the traditional high-volatility solvents indicating the potential of glycol ethers to form secondary organic aerosol (SOA). This is the first work on SOA formation from glycol ethers. The impact of molecular structure, specifically –OH, on SOA formation from glycol ethers and related ethers are investigated in the work. Ethers with and without –OH, with methyl group hindrance on –OH and with –OH at different location are studied in the presence of NO_X and under "NO_X free" conditions. Photooxidation experiments under different oxidation conditions confirm that the processing of ethers is a combination of carbonyl formation, cyclization and fragmentation. Bulk SOA chemical composition analysis and oxidation products identified in both gas and particle phase suggests that the presence and location of –OH in the carbon bond of ethers determine the occurrence of cyclization mechanism during ether oxidation. The cyclization is proposed as a critical SOA formation mechanism to prevent the formation of volatile compounds from fragmentation during the oxidation of ethers. Glycol ethers with $–CH_2–O–CH_2CH_2OH$ structure is found to readily form cyclization products, especially with the presence of NOx, which is more relevant to urban atmospheric conditions than without NOx. Glycol ethers are evaluated as dominating SOA precursors among all ethers studied. It is estimated that the contribution of glycol ethers to anthropogenic SOA is roughly 1% of the current organic aerosol from mobile sources. The contribution of glycol ethers to anthropogenic SOA is roughly 1% of the current organic aerosol from mobile sources and will play a more important role in future anthropogenic SOA formation.

* Corresponding author. University of California, Riverside, Department of Chemical and Environmental Engineering, Riverside, CA 92507, USA.
E-mail address: dcocker@engr.ucr.edu (D.R. Cocker).

https://doi.org/10.1016/j.atmosenv.2017.12.025
Received 23 May 2017; Received in revised form 7 November 2017; Accepted 16 December 2017
Available online 05 February 2018
1352-2310/

1. Introduction

Glycol ethers are compounds with formula of $R-(OCH_2CH_2)_n-OR'$ (n = 1,2,3) (EPA, 2000). They are widely used as solvents in consumer product industries including architecture coatings, cleaning products, adhesives, pesticides and pharmaceuticals (EPA, 2000; Singer et al., 2006; Fromme et al., 2013). Previous studies suggest that short chain glycol ethers are sufficiently volatile to be available in the atmosphere (Cooper et al., 1995; Zhu et al., 2001; Singer et al., 2006) and in indoor air (Gibson et al., 1991; Nazaroff and Weschler, 2004; Choi et al., 2010; Wieslander, and Norbäck, 2010a, b). A recent study foundglycol ethers exempted as low vapor pressure-volatile organic compounds (LVP-VOCs) were also sufficiently volatile to evaporate (Võ and Morris, 2014). LVP-VOCs, classified as compounds with > 12 carbons, vapor pressure < 0.1 mmHg, or by boiling point (varies by agency) are currently exempted by US Environmental Protection Agency (EPA), California Air Resources Board (CARB) and Ozone Transport Commission (OTC) in consumer product VOC regulation. The US EPA classified glycol ethers as hazardous air pollutants under the 1990 Clean Air Act Amendments. It is estimated that emission of known glycol ethers in California will be 13.44 tons per day in 2020 a based on databases provided by the CARB and industrial sectors (Cocker et al., 2014). Therefore, it is important to understand the primary and secondary impact of glycol ethers on air quality and human health.

The oxidization of intermediate and semi-volatile organic compounds (IVOCs and SVOCs) is predicted to be a larger source of global aerosol production than that of traditional volatile organic compounds (VOCs) (Pye and Seinfeld, 2010). A typical type of IVOC is long carbon chain alkanes. Ethers are less volatile and more reactive during oxidation than alkanes with the same amount of carbons (Pankow and Asher, 2008; Mellouki et al., 2003). Six to eight carbon glycol ethers, such as diethylene glycol monoethyl ether and diethylene glycol monobutyl ether, are in the IVOC range (Donahue et al., 2012). However, SOA formation from glycol ethers is seldom investigated compared with other well-known IVOCs or SVOCs (semi-volatile organic compounds) such as terpenes, polycyclic aromatic hydrocarbons and long chain alkanes.

Gas phase oxidation of ethers and simple glycol ethers (n = 1 in $R-(OCH_2CH_2)_n-OR'$, R' = H or alkyl group)) is well documented in previous studies (Tuazon et al., 1991; Wallington and Japar, 1991; Eberhard et al., 1993; Mellouki et al., 1995; Johnson, and Andino, 2001; Mellouki et al., 2003; Orlando, 2007; Tommaso et al., 2011). It is clear that forming alkoxy radical through H-abstraction by ·OH, mostly at α-carbon H, is a dominant initial step of ether photooxidation (Aschmann, and Atkinson, 1998). Alkoxy radicals may undergo further fragmentation by carbon-carbon bond scission to form formates, ketones and aldehydes (Mellouki et al., 2003). Organic carbonates (e.g. dimethyl carbonate) are also observed as important products from oxidation of ethers (Wenger et al., 1999; Geiger and Becker, 1999; Platz et al., 1999). Further, hydroperoxides oxidation product formation is expected in absence of NO_X (Jenkin et al., 1993; Sehested et al., 1996). The presence of NO_X leads to nitrate formation including peroxynitrate and peroxyacyl nitrate (Aschmann and Atkinson, 1999; Orlando, 2007; Malanca et al., 2009) and affects alkoxy radical decomposition (Collins et al., 2005; Orlando, 2007). Reaction with NO_3 radical may also contribute to a small extent ofether removal during night-time, while photolysis and reaction with O_3 are negligible (Chew et al., 1998; Mellouki et al., 2003). This study focuses on the daytime chemistry of ether with OH radical.

While early studies only concentrated on gas phase oxidation from glycol ethers, it is noted that a cyclic product is observed by Stemmler et al. (1996) from the oxidation of a simple glycol ether (2-Ethoxyethanol). Cyclization reduces fragmentation of ethers thereby leading to higher molecular weight products, which may partition into the particle phase, especially during the oxidation of glycol ethers with high initial molecular weight and low volatility (e.g. n > 1, in $R-(OCH_2CH_2)_n-OR'$).

Organic nitrate formation from NO_X and peroxide radical may compete with the cyclization pathway (Stemmler et al., 1996). Espada and Shepson (2005) discussed -OR′ impact on ether organic nitrate product stability and yields. However, previous studies were mostly conducted with NO_X concentrations higher than hundreds ppb, which is less atmospherically relevant (Stemmler et al., 1996; Aschmann and Atkinson, 1999; Orlando, 2007). It is important to study ether oxidation under atmospherically relevant NO_X conditions in order to extend laboratory data to ambient prediction.

In this study, the potential of SOA formation from glycol ethers and the related ethers is investigated under NO_X free and with NO_X condition. SOA yields and chemical compositions from different ethers are compared to explore the effect of molecular structure on SOA formation from glycol ethers. Further, the influence of NO and hydroxyl radical (·OH) on SOA formation from ethers is discussed. Finally, the contribution of ethers to global SOA formation is evaluated.

2. Methods

2.1. Environmental chamber

The UC Riverside/CE-CERT indoor dual 90 m^3 environmental chambers were used in this study and are described in detail elsewhere (Carter et al., 2005). Experiments were all conducted at dry conditions (RH < 0.1%), in the absence of inorganic seed aerosol, and with temperature controlled to 27 ± 1 °C. Positive differential pressure (~0.02″ H_2O) was maintained and blacklights were used as previously described (Li et al., 2015).

A known volume of high purity liquid semivolatile ethers (boiling point > 150 °C) were injected through a glass manifold inside a temperature controlled oven (oven temperature 80–120 °C adjusted according to the physical properties of ethers) and flushed into the chamber with pure N_2. Volatile ethers (boiling point < 150 °C) were injected through a heated glass injection manifold system instead of a manifold inside the oven. NO and hydrogen peroxide (H_2O_2) injection followed previous work (Li et al., 2015; Li et al., 2016a). Pure irradiation experiments, with cleaned bag refilled with pure air, were conducted in between the ether experiments to ensure the background aerosol formed during 8 h photooxidation is less than 2 μg/m^3. The chamber is cleaned thoroughly (aerosol number concentration (< 5/cm^3) and mass concentration (< 0.005 $\mu m^3/cm^3$)) after each experiment and flushed with compressed air until the next experiment (> 8 h).

2.2. Particle and gas phase analysis

Ether decay was measured by a pair of Agilent 6980 (Palo Alto, CA) gas chromatographs (GC) equipped with flame ionization detectors (FID) or Selected Ion Flow Tube-Mass Spectrometry (SIFT, Syft Technology, Voice 200®). NO_X measurement followed early studies (Li et al., 2015; Li et al., 2016a).

Aerosol volume growth was measured and calculated following previous work (Li et al., 2015). Evolution of particle-phase chemical composition was measured by a High Resolution Time of Flight Aerosol Mass Spectrometer (HR-ToF-AMS; Aerodyne Research Inc.) (Canagaratna et al., 2007; DeCarlo et al., 2006). The operation conditions and data analysis toolkit of HR-ToF-AMS followed Li et al. (2016b). Elemental ratios for total organic mass, oxygen to carbon (O/C), and hydrogen to carbon (H/C) were determined using the elemental analysis (EA) technique (Aiken et al., 2007, 2008).

2.3. Ether selection

A series of ethers (Fig. 1) are identified and used to investigate the impact of molecular structure on SOA formation from glycol ether

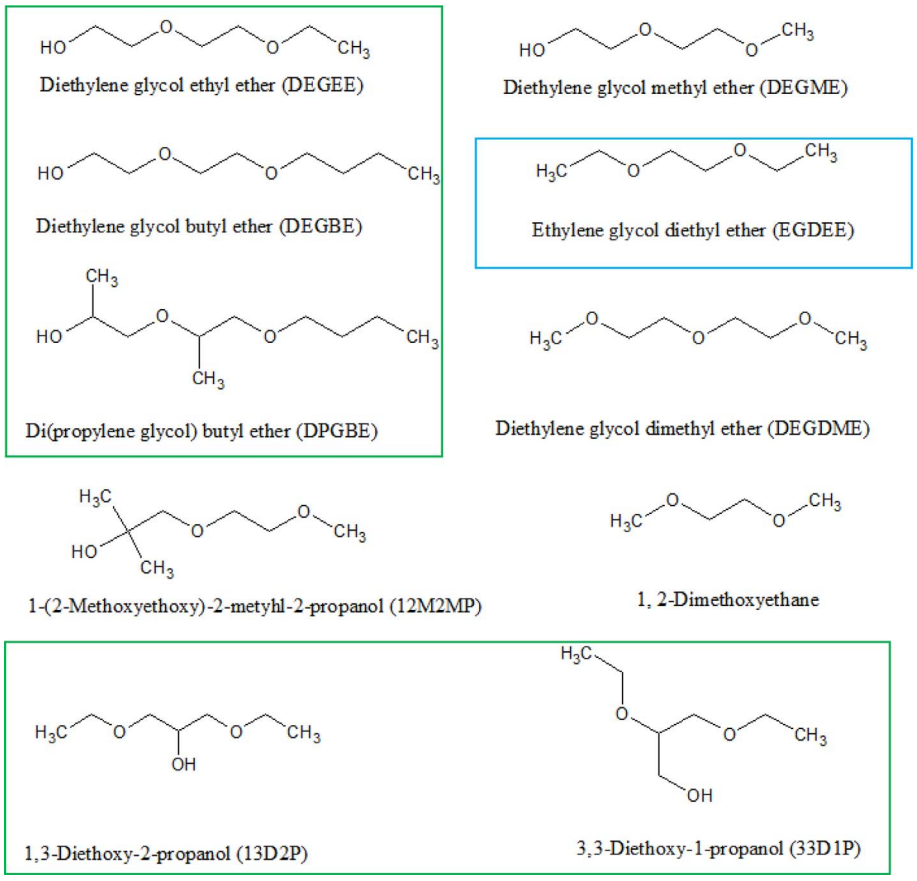

Fig. 1. Molecular structure of ethers investigated. Note: Green boxes indicate precursors with high SOA formation potential or $M_o > 15\ \mu g{\cdot}m^{-3}$; and similarly blue dashed box indicates precursor with media SOA formation potential or $M_o = [3, 15]\ \mu g{\cdot}m^{-3}$; unboxed precursors form insignificant SOA with M_o less than $3\ \mu g{\cdot}m^{-3}$. (For interpretation of the references to color in this figure legend, the reader is referred to the Web version of this article.)

($R-(OCH_2CH_2)_n-OR'$). Diethylene glycol ethyl ether (Sigma-Aldrich, 99%, DEGEE) and diethylene glycol butyl ether (Sigma-Aldrich, ≥99%, DEGBE) are two basic ethers focused in the current study due to their wide application in consumer products, low volatility and therefore higher potential to SOA formation. Diethylene glycol methyl ether (Sigma-Aldrich, ≥99%, DEGME) is selected to study the impact of carbon chain length in R-on SOA formation from glycol ether. Ethylene glycol diethyl ether (Sigma-Aldrich, 98%, EGDEE) is used to compare with DEGEE in order to demonstrate the importance of –OR′ or –OH to SOA formation from glycol ether. Diethylene glycol dimethyl ether (Sigma-Aldrich, 99.5%, DEGDME) an isomer of DEGEE, is used to evaluate the role of alkoxy group ($-OC_nH_{2n+1}$, R′ = Alkyl group) to SOA formation from glycol ether compared with–OH (R′ = H). Di (propylene glycol) butyl ether (eNovation Chemicals, > 95%, DPGBE) and 1-(2-Methoxyethoxy)-2-methyl-2-propanol (Sigma-Aldrich, > 98%, 12M2MP), comparing with corresponding glycol ethers (DEGBE and DEGME, respectively), are used to investigate the $–CH_3$ hindrance effect on –OH and its role to SOA formation. Further, 1, 3-diethoxy-2-propanol (Sigma-Aldrich, Aldrich^{CPR} 13D2P) and 3, 3-diethoxy-1-propanol (Sigma-Aldrich, 98%, 33D1P) are identified to study the influence of –OH position on ether oxidation. 1, 2-Dimethoxyethane (Sigma-Aldrich, 99.5%) represents a simple glycol ether in this study to compare with earlier studies. Three experimental schemes used in this study are as followed: 1) NO_X free (H_2O_2 only): ether + 1 ppm H_2O_2; 2) in presence of NO_X (NO_X only): ether + ~20 ppb NO; 3) NO_X with sufficient OH (H_2O_2-NO): ether + 1 ppm H_2O_2 + ~20 ppb NO (Table S1).

3. Results

3.1. SOA formation in absence of NO_X

The SOA formation of glycol ethers is investigated under NO_X free condition (described as H_2O_2-only hereafter). SOA mass concentration and yield are both used to evaluate the SOA formation potential from ethers.

3.1.1. SOA mass concentration

A substantial amount of SOA is formed during the photooxidation of two basic glycol ethers studied (DEGEE $M_O = 18.9–48.3\ \mu g{\cdot}m^{-3}$ and DEGBE $M_O = 154–177\ \mu g{\cdot}m^{-3}$, M_O is the organic aerosol mass concentration formed in the end of each experiment as described by Odum et al. (1996)). A smaller amount of SOA is formed from DEGME, indicating that the lengths of carbon chain in R-impact SOA formation under H_2O_2-only condition. EGDEE with similar molecular structure to DEGEE but without –OR′ structure, forms less amount of SOA ($4.4–10.3\ \mu g{\cdot}m^{-3}$) than DEGEE (Fig. 2). The reaction rate constant of EGDEE with ·OH is similar to that of DEGEE (Table S2) supporting that a similar amount of ether is reacted under the similar initial ·OH conditions. This suggests that the existence of –OH or –OR′ in glycol ether structure promotes the formation of less volatile products during the oxidation of glycol ether. DEGDME, an isomer of DEGEE, contains alkoxy group instead of −OH in glycol ether. An insignificant amount of SOA is formed from DEGDME. It indicates that the existence of –OH rather than alkoxy group in glycol ether structure activates the formation of less volatile products during the ether oxidation.

The importance of –OH on SOA formation from ethers is confirmed by blocking –OH using methyl groups near –OH. DPGBE, compared with DEGBE, has two more methyl groups attached to $-(OCH_2CH_2)_n-$ carbon, at α and γ position of –OH respectively. DPGBE ($77.7–131\ \mu g{\cdot}m^{-3}$) shows a slight SOA decrease under similar amount of ether consumption (Fig. 2 and Table S1). SOA formed from 12M2MP, which has two more methyl groups at α position of –OH than DEGME, is comparable to that from DEGME. This suggests that adding methyl group to carbons in $-(OCH_2CH_2)_n-$ exerts only a small impact on SOA

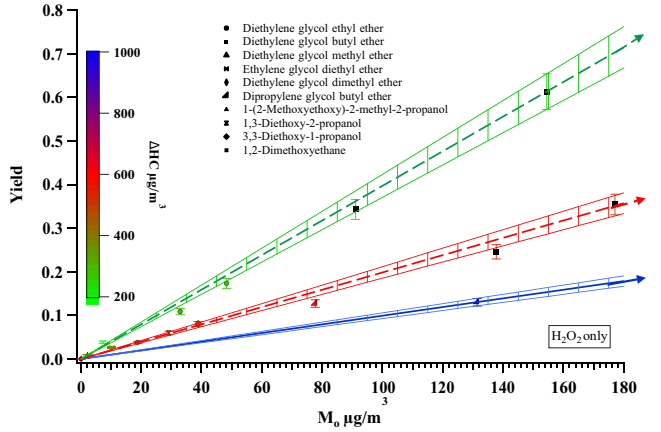

Fig. 2. SOA yield from glycol ethers and relative ethers in absence of NO_x. Experimental data points are colored proportional to the amount of ether reacted (ΔHC) with high, median and low ΔHC marked in blue, red and green; green dash-dotted line, red dashed line and blue solid line correspond to 40 ppb (263.6 μg·m^{-3}), 80 ppb (527.2 μg·m^{-3}), and 160 ppb (1054.4 μg·m^{-3}) of DEGBE reacted). The uncertainty of SOA yield associated with 10 replicate calibration experiments is < 6.65%. Both data points and the representative lines with slope = 1/ΔHC are marked with an error bars. Diethylene glycol methyl ether, diethylene glycol dimethyl ether, 1-(2-methoxyethoxy)-2-methyl-2-propanol and 1,2-dimethoxyethane forming insignificant SOA (M_o < 3 μg·m^{-3}) overlapped near the origin. (For interpretation of the references to color in this figure legend, the reader is referred to the Web version of this article.)

formation from ethers under H_2O_2-only conditions.

The role of –OH on SOA formation from ethers is investigated by varying the position of –OH in the ether molecular structure. SOA formations from 13D2P and 33D1P are in between the amount of SOA formed from DEGEE and DEGBE when similar mole amount of ethers is reacted (Fig. 1 and Table S1). This agrees with the decrease of vapor pressure with the increase of -CH_2- group number (Pankow and Asher, 2008) assuming that –OH located in the middle of carbon chain dose not significantly change the reaction mechanism compared with –OH is in the terminal of the chain. This suggests that for the ethers studied in this work, the location of –OH in the ether chain exerts insignificant impact on major SOA formation mechanism from ethers. Insignificant amount of SOA is formed during the photooxidation of 1, 2-dimethoxyethane consistent with these volatile products proposed in earlier study (Geiger and Becker, 1999).

3.1.2. SOA yield and ΔHC

SOA yield is calculated as a mass ratio of SOA formed to ether reacted during the photooxidation according to Odum et al. (1996) work. The uncertainty of SOA yield associated with 10 replicate calibration experiments (*m*-xylene and NO) is < 6.65%. The relationship between SOA yield and mass loading (M_o) during the photooxidation of ethers in absence of NO_X is shown (Fig. 2). It is noted that the SOA yields of ethers depend on the amount of ether precursor reacted in addition to mass loading. The initial conditions of all the experiments in Fig. 2 are 1 ppm of H_2O_2 and 40–160 ppb ethers. Lower SOA yield is observed with higher amount of ether consumption. This is an artifact of plotting mathematically correlated variables where the y-axis is 1/ΔHC of the x-axis.

Therefore, SOA formation potential of ethers is evaluated by comparing the amount of SOA formed under similar ΔHC instead of SOA yield under similar mass loading. It is concluded that the SOA formation potential is ranked as DEGBE > DPGBE > 33D1P > 13D2P > DEGEE > EGDEE > other ethers. No additional SOA yield comparison is addressed among ethers forming insignificant (< 3 μg·m^{-3}) SOA, except for DEGME, which forms a significant amount of SOA under NOx-only conditions (Section 3.4). The following chemical composition analysis (Section 3.2 and 3.3) focuses on ethers that have significant SOA formation.

3.2. SOA chemical composition

3.2.1. Precursor carbon number normalized elemental ratio

Elemental ratio analysis (Aiken et al., 2007, 2008) provides a mole based SOA chemical composition to probe SOA formation mechanisms (Heald et al., 2010; Chhabra et al., 2011). The change of H/C vs. O/C from precursor to SOA is discussed in supplemental material (S.1), which demonstrates the impact of precursor elemental composition on SOA elemental composition. It is noted that the mole based elemental ratio of SOA may bias the comparison of oxidation between different precursors, especially when precursors have different number of carbons (Li et al., 2016a). Li et al. (2016a) developed the aromatic ring-based elemental ratio to compare the similarities and differences of SOA chemical compositions produced from aromatic hydrocarbons with different alkyl substitutes. Here, precursor carbon number normalized elemental ratio parameters (*O/M, H/M and -Δ(H/M)*) derived from elemental ratio are introduced (Eq-1 ~ 3) in this section to compare the extent of the oxidation for SOA precursors with various carbon number.

$$O\big/_M = n_c \times O\big/_C \tag{1}$$

$$H\big/_M = n_c \times H\big/_C \tag{2}$$

$$-\Delta\left(H\big/_M\right) = \left(H\big/_M\right)_{pre} - \left(H\big/_M\right)_{SOA} \tag{3}$$

where *O/M* and *H/M* are precursor carbon number normalized elemental ratios; *M* stands for the mole of ether precursor consumed during the photooxidation; *O/C* and *H/C* are traditional mole based elemental ratios (Aiken et al., 2007, 2008), meaning that *O/C* or *H/C* is the mole ratio of oxygen to carbon or hydrogen to carbon in the precursor or the secondary organic aerosol (SOA); n_c is the number of carbons in ether precursor; $(H/M)_{pre}$ and $(H/M)_{SOA}$ are *H/M* of the ether precursor and its SOA, respectively; *-Δ(H/M)* is the difference between ether precursor and its SOA in *H/M*.

O/M and *-Δ(H/M)* of SOA formed from all ethers studied are similar with an average value of 4.35 ± 0.35 and 4.10 ± 0.32, respectively (Fig. 3). *O/M* represents the average oxygen content of SOA and *-Δ(H/M)* represents the hydrogen loss of the precursor during oxidation assuming that oxidized products have the same number of carbons as their corresponding precursor. That means SOA formation from ethers can be estimated by an oxidation process that adds oxygen until the SOA products contain an average ~4 oxygen per precursor molecular by losing ~4 hydrogen from the precursor. Most of the ethers that form SOA in this work start with precursors with 3 oxygen and a double bond equivalent (DBE) = 0, except for EGDEE (2 oxygen and DBE = 0). Aliphatic carbon oxidized into carbonyl can explain a loss of 2 hydrogens and a gain of 1 oxygen. Losing 4 hydrogen while gaining 2 oxygen during the photooxidation of EGDEE can be readily explained by two aliphatic carbon oxidized into carbonyls. However, ether precursors that contain 3 oxygen must have another step to lose 2 additional hydrogen without oxygen addition to form the average SOA composition measured. This addition step suggests the importance of cyclization pathway to SOA formation from ethers, which loses 2 hydrogen without increasing oxygen. All ethers (except EGDEE) that formed measurable SOA contained an –OH functional group. This suggests that importance of –OH to cyclization and therefore the overall SOA formation. The similar SOA *O/M* values provide a general estimation for the required functionalization steps needed for an ether precursor to form SOA, especially for precursors containing 6–10 carbons. OS_c and carbon number (Fig. S1b) suggest that ether oxidation products are among SV-OOA and LV-OOA (Kroll et al., 2011). The vapor pressure of products formed from the mechanism proposed above (aliphatic carbon to carbonyl coupled with cyclization) ranges from 10^{-3} to 10^{-6} atm based on SIMPOL prediction (Pankow and Asher, 2008) yielding saturation vapor pressure (C*) on the order of 10^5 μg·m^{-3} (Table S3). This

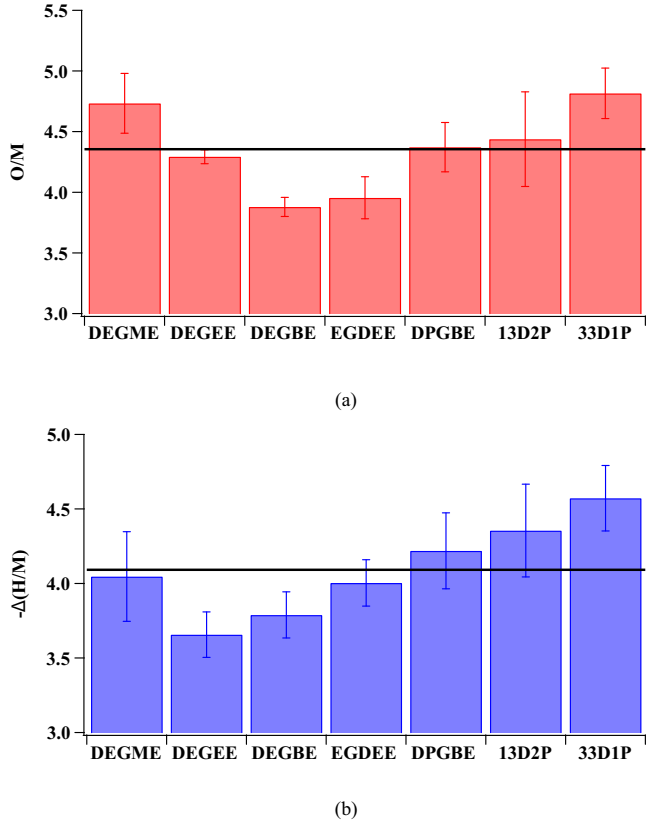

Fig. 3. Molecular based chemical composition of SOA formed during the oxidation of glycol ethers and relative ethers in absence of NO_x: a) *O/M*; b) $-\Delta$ *(H/M)*. Horizontal black lines are average *O/M* and *Δ(H/M)* of SOA formed from ethers listed in graphs. The error bars represents one standard deviation of *O/M* and *Δ(H/M)* during the photooxidation of each experiment.

suggests that cyclization products require additional reactions like oligomerization to form SOA from ethers.

The influence of individual reaction on *O/M* increase ranks from high to low as [fragmentation without oxygen loss] > [carbonyl formation (+1)] > [fragmentation with one oxygen loss] > [cyclization (+0)]; the influence of these reactions on *-Δ(H/M)* increase ranks from high to low as cyclization = carbonyl formation (+2) > fragmentation. It is noted that fragmentation associates with carbonyl formation on the terminal carbon. A decrease in *O/M* and an insignificant decrease in *-Δ(H/M)* from DEGME to DEGEE to DEGBE is possibly due to preferred cyclization over carbonyl formation when the R–substitute carbon chain is longer. The favored location of carbonyl formation may shift to the alky substitute while the electron donating property of n-alkyl substitute increases with the number of carbons. Therefore, the possibility of cyclization through γ−carbon of –OH increases as the preference of carbonyl formation decreases. The significantly higher *O/M* and *-Δ(H/M)* of 33D1P than the average indicates that 33D1P are more oxidized than other ethers, possibly due to a higher amount of carbonyl formation. Located in the middle carbon chain, –OH is closer to a greater number of carbons on the carbon chain therefore promoting more carbonyl formation compared to terminal –OH. *O/M* and *-Δ(H/M)* of SOA formed from DPGBE are both slightly higher than those from DEGBE while DPGBE has lower SOA formation than that of DEGBE. This suggests that carbonyl formation with fragmentation is favored during SOA formation from DPGBE than that of DEGBE. The lower *O/M* in EGDEE compared with other ethers is due to a fewer amount of oxygen contained in initial ether precursor. Another detailed comparison in section S2 using f_{CO2}^+ vs f_{C2H3O}^+ suggests similar SOA formation pathways from different ethers. Overall, the chemical composition of SOA confirms that SOA formation from ethers is a combination of fragmentation, carbonyl formation, cyclization and oligomerization. The cyclization pathway is critical to SOA formation from glycol ethers.

Table 1
Representative particle (HR-TOF-AMS) and gas (SIFT-MS) phase peaks in SOA formed from ether photooxidation.

m/z	Particle phase		Gas phase				
	73	47/61/89	75	73	104	M_p-2	M_p+29
	Fragment		SIFT Ion Source				
	$C_3H_5O_2^+$	$C_nH_{2n+1}O_2^+$	(H_3O^+)	(NO^+)	(NO^+)	(H_3O^+ & NO^+)	(NO^+)
DEGME	✓	✓	✓	✓	✓	–	✓
DEGEE	✓	✓	✓	✓	✓	✓	✓
DEGBE	✓	✓	✓	✓	✓	✓	✓
EGDEE	–	✓	✓	*	✓	–	–
DPGBE	–	✓	✓	*	–	✓	–
13D2P	-[a]	✓	✓	*	✓	✓	–
33D1P	-[a]	✓	*	✓	–	✓	*

Note: ✓: newly formed during the oxidation of ethers; *: signal masked by high precursor peak; -:Not observed or not significant (denote with a). M_p: major m/z peaks from precursor.

3.3. Representative products in particle and gas phase

3.3.1. Representative products in particle phase

Functional groups of ether oxidation products in particle phase is inferred from fragments generated from HR-TOF-AMS. A large amount of $C_3H_5O_2^+$ fragments (m/z 73) is observed for ethers with $–CH_2–O–CH_2CH_2OH$ structure (Table 1, DEGBE, DEGEE and DEGME). However, less m/z 73 is observed in SOA formed from EGDEE, DPGBE, 13D2P and 33D1P than ethers with $–CH_2–O–CH_2CH_2OH$ (Table 1). The absence of $C_3H_5O_2^+$ in SOA formed from EGDEE confirms that $C_3H_5O_2^+$ is not associated with carbonyls, which can be formed without –OH. $C_3H_5O_2^+$ is expected to associate with a ring structure such as the dioxolane group as proposed by Stemmler et al. (1996). SOA formed from DPGBE also contains cyclization structure but with additional $–CH_3$ on the ring ($C_4H_7O_2^+$ at m/z 87). A smaller fraction of m/z 73 while a larger fraction of m/z 61 ($C_2H_5O^+$) is formed during the oxidation of 13D2P and 33D1P suggesting cyclization is less favored than carbonyl formation compared with DEGEE. Therefore, the presence of –OH determines the possibility of cyclization and the location of –OH determines branching ratio of cyclization pathway.

General aldehyde, ketone, acid and ester fragments, such as CHO^+ (m/z 29), $C_2H_2O^+$ (m/z 42), $C_2H_3O^+$ (m/z 43), CHO_2^+ (m/z 45), C_2HO^+ (m/z 41) and $C_2H_4O_2^+$ (m/z 60) (McLafferty and Tureček, 1993) are observed in SOA as oxidation products for all ethers along with common fragments associated with ether structure (CH_3O^+ (m/z 31) and $C_2H_5O^+$ (m/z 45)) (Fig. 4a). $C_nH_{2n+1}O_2^+$ fragments (n = 1, 2 and 4, corresponds to the number of carbon in R-of ether) are observed in all ethers with significant SOA formation in this study (Table 1). These fragments originate from the oxidation of carbon in R-adjacent to –O– since the saturated oxygen atom of the ester group can act as a site to which a hydrogen atom can be transferred during electronic ionization (McLafferty and Tureček, 1993). It is consistent with Section S.2. This finding suggests that the oxidation of R-contributes to SOA formation in addition to cyclization.

3.3.2. Representative peaks in gas phase

Gas phase composition during the oxidation of ether is measured by SIFT-MS. SIFT-MS utilizes three ion sources (H_3O^+, NO^+ and O_2^+) to realize soft chemical ionization providing multiple fingerprints for the same compound and therefore facilitates the identification of isomer species. For example, ketone and aldehyde may show the same peak from

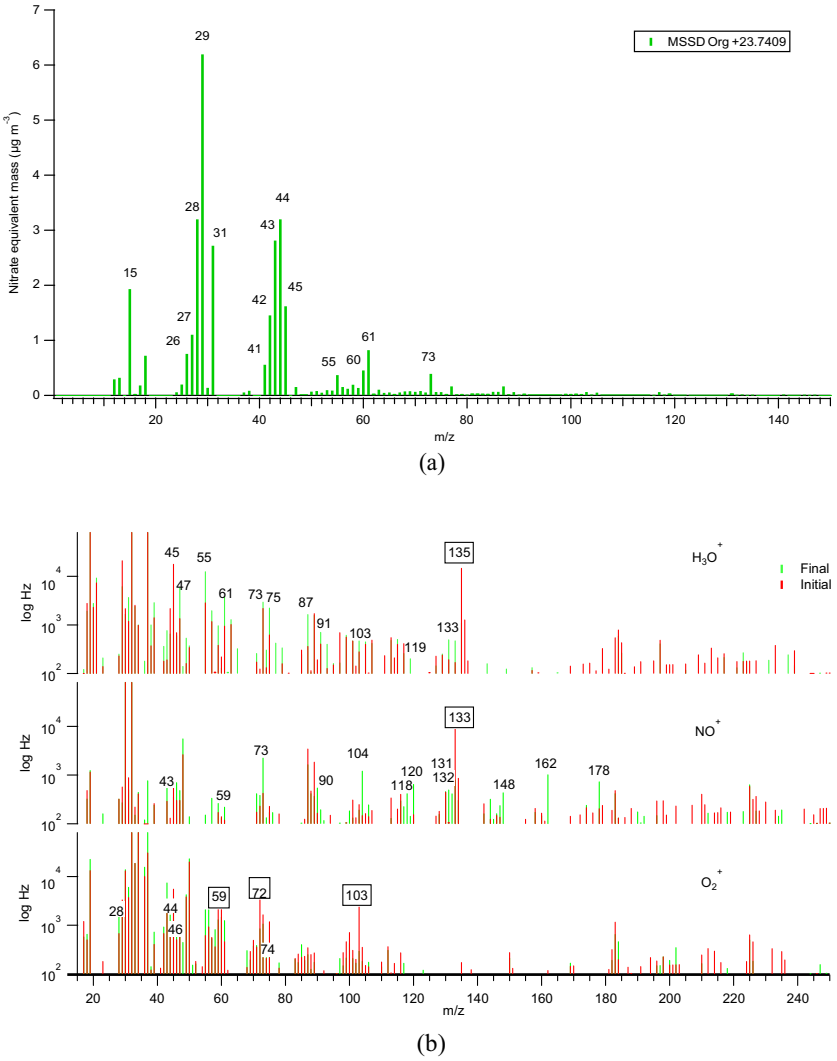

Fig. 4. Particle phase (a) and gas phase (b) mass spectrum during the photooxidation of DEGEE in absence of NO_x (1991A). Top, middle and bottom panel in (b) stands for mass spectrum ionized by H_3O^+, NO^+ and O_2^+ correspondingly. Final mass spectrum is showed as green bars underneath initial mass spectrum showed as red bas. The boxed m/z is the major peaks in ether precursors. (For interpretation of the references to color in this figure legend, the reader is referred to the Web version of this article.)

H_3O^+ ionization (M+1) but show different peaks in NO^+ ionization (ketone: M-1; aldehyde: M+30, M stands for the molecular weight of the compound) (Španěl et al., 1997). The following discussion shows m/z of mass spectrum peak from different ions as (m/z_{H3O}^+, m/z_{NO}^+ (, m/z_{O2}^+)) in which the subscript refers to the ion source. The m/z peak from O_2^+ is not presented since the high ionization energy of O_2^+ leads to a large amount of fragment peaks instead of molecular peaks.

Cyclic products are found to form from the oxidation of select ethers (75, 73) indicating that the formation of cyclic ether such as 1,3-dioxolane and (75, 104) associates with ethyl formate. It is concluded from the mass spectrum that cyclic ether is found during the oxidation of DEGME, DEGEE and DEGBE while ethyl formate is dominating in oxidation products at m/z 75 (H_3O^+) formed from EGDEE and 13D2P (Table 1). Either a m/z 75 (H_3O^+) or a m/z 73 (NO^+) signal is observed for 33D1P and DPGBE molecule prior to oxidation commencing that masks observation of cyclic ether formation (75, 73). It is noted that the observed m/z 75 (H_3O^+) during DPGBE oxidation is not associated with ethyl formate formation since the corresponding m/z 104 (NO^+) signal is not observed. m/z 73 (NO^+) is observed to form during the oxidation of 33D1P. Therefore, cyclic ethers are likely present after oxidation of DPGBE and 33D1P (Table 1).

(M_p-2, M_p-2) (M_p denotes a major m/z molecular peak from precursor) is considered as another important cyclic structure. However, (M_p-2, M_p+29) indicates the formation of aldehyde substituting for –OH. M_p-2 peaks observed for DEGEE and DEGBE oxidation are a combination of aldehyde and cyclic ether formation. Peaks from cyclization products (M_p-2, M_p-2) are also observed during the oxidation of 33D1P. Cyclic ether largely contributes to M_p-2 peaks during the oxidation of DPGBE and 13D2P. Insignificant (M_p-2, M_p-2) compared with (M_p-2, M_p+29) during the oxidation of DEGME suggests that cyclization without fragmentation is less favored than aldehyde formation. M_p-2 peaks are not observed from the oxidation products of EGDEE due to the lack of –OH structure. Overall, cyclization products in gas phase during the oxidation of ethers with –OH function group can be inferred from SIFT-MS.

A typical mass spectrum of gas phase products formed from the oxidation of DEGEE is presented in Fig. 4b. Products such as glycol monoformate (91,120) and glycolaldehyde C_2H_4O (61, 90) are observed during the oxidation of DEGEE. Peaks associated with formate and aldehyde formation are observed during the oxidation of all ethers studied, consistent with previous studies (Tuazon et al., 1998; Geiger and Becker, 1999).

3.4. Influence of NOx-only (on H_2O_2) on SOA formation from ethers

SOA formation from the photooxidation of ethers in presence of NO_X conditions (initial NO = 15–25 ppb) are investigated (Table S1) to evaluate the impact of NO_X on SOA formation. Less SOA mass is formed

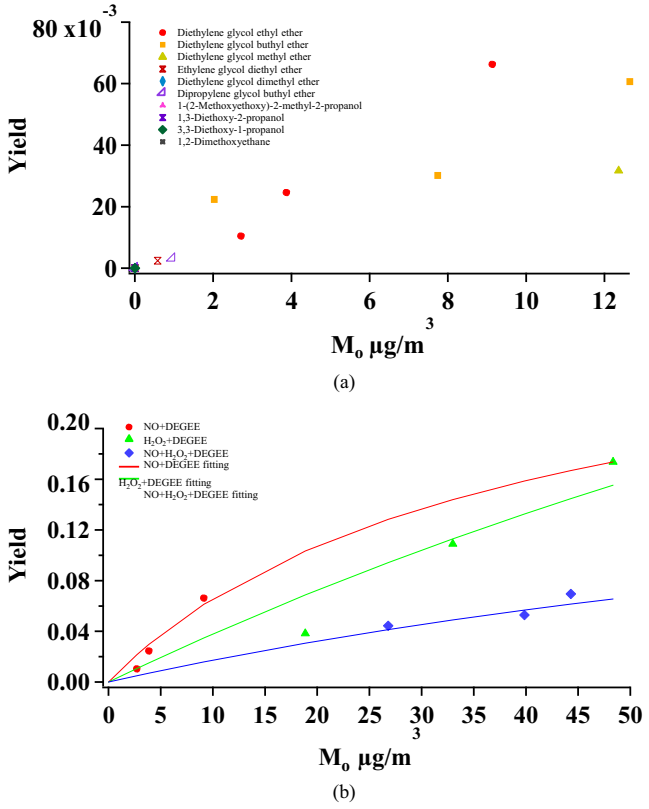

Fig. 5. Comparison of SOA yield during the photooxidation of a) ethers under NO_X-only conditions b) from DEGEE under different reactivity. Tentative two product model fitting for SOA formation from DEGEE under different conditions (NO_X + DEGEE $\alpha_1 = 0.207$, $K_{om,1} = 0.035$, $\alpha_2 = 0.145$, $K_{om,2} = 0.009$; H_2O_2 + DEGEE $\alpha_1 = 0$, $\alpha_2 = 0.800$, $K_{om,2} = 0.005$; NO_X + H_2O_2 + DEGEE $\alpha_1 = 0$, $\alpha_2 = 0.242$, $K_{om,2} = 0.008$).

from ethers under NO_X-only conditions compared with H_2O_2-only conditions due to a lower OH concentration and ether precursor consumption (Table S1). Larger amounts of SOA ($> 2\,\mu g{\cdot}m^{-3}$) is formed during the oxidation of DEGEE, DEGBE and DEGME (Fig. 5a) than that formed during the oxidation of EGDEE, DPGBE, 13D2P, 33D1P and 12M2MP ($0.01 \sim 1\ \mu g{\cdot}m^{-3}$). It is noted that 12M2MP forms much less SOA compared with DEGME under NO_X-only condition. This suggests that adding methyl group to carbons in $-(OCH_2CH_2)_n-$ alter the preference of ether reaction pathways, especially in presence of NO_X. It is possible that extra methyl group on carbon chain suppresses intermolecular cyclization associate with –OH, which is expected to reduce the fragmentation of ethers. It is noted that adding methyl groups next to –OH increases the overall reaction rate constant of an ether (Porter et al., 1997). The hindrance effect of methyl groups on the intermolecular cyclization related to –OH is possibly due to a decrease of H-abstraction at γ position carbon when more methyl groups are added next to $-$OH diminishing the cyclization reaction pathways associated with H-abstraction at γ position carbon.

No significant correlations are observed between SOA formation and k_{OH}, final NO concentration, organic nitrate formation (< 5% of total SOA mass) and hydrocarbon consumption. However, molecular structure of the precursor directly impacts SOA formation in the presence of NO_x. It is noted that, under the NO_X-only condition, SOA formation remains significant from ethers with–CH_2–O–CH_2CH_2OH. A higher abundance of m/z 73 and lower m/z 61 is found in SOA formed during the photooxidation of DEGEE under NO_X-only condition (Fig. S3a, Table 2) compared with under H_2O_2-only conditions (Fig. 4a). This highlights a greater importance of cyclization to SOA formation under NO_X-only conditions. The SOA formation of ethers without –CH_2–O–CH_2CH_2OH, including DPGBE, EGDEE, 13D2P and 33D1P in the absence of NO_X, depends more on carbonyl formation than

Table 2
Representative HR-TOF-AMS peaks from DEGEE oxidation under different conditions.

Oxidation Condition	m/z 73	m/z 61	m/z 87
	$C_3H_5O_2^+$	$C_2H_3O_2^+$	$C_4H_7O_2^+$
H_2O_2	1.18%	2.47%	–
NO	4.7%	–	0.80%
H_2O_2 + NO	2.44%	2.31%	0.84%

Note: : not significant.

cyclization (Table 1, Section 3.2, 3.3). The presence of NO further promotes the carbonyl formation by enhancing the rate of $RO_2{\cdot}$ to RO· conversion. However, the NO promotion on carbonyl formation coexists with fragmentation (Stemmler et al., 1996). Only ether precursors with –CH_2–O–CH_2CH_2OH to from cyclic products could protect the molecule from becoming more volatile by fragmentation. Therefore, –CH_2–O–CH_2CH_2OH structure, which is critical to cyclization, determine SOA formation from ethers under NO_X-only condition.

3.5. Relationship between oxidation and SOA formation

SOA formation during the photooxidation of DEGEE under different oxidation conditions are studied (NO_X-only, H_2O_2-only and H_2O_2-NO_X; Table S1, Fig. 5b). The two-product model (Odum et al., 1996) is used to compare the SOA yield under similar mass loadings (Fig. 5b). The SOA yield of DEGEE under different conditions shows a trend of $yield_{NOX\text{-}only} > yield_{H2O2} > yield_{H2O2\text{-}NOX}$, inversely correlating with ·OH concentration and extent of oxidation. This suggests that further oxidation of ether forms more volatile compounds consistent with similar observations in Sections 3.1.2 and 3.4. A recent study also suggests that continued oxidation of SOA may lead to fragmentation and therefore lower SOA mass (Hall et al., 2013).

Chemical bulk compositions of SOA formed from DEGEE under different conditions show an oxidation trend of $OSc_{,NOx\text{-}only}$ $(-0.82 \pm 0.20) < OSc_{,H2O2\text{-}only}$ $(-0.29 \pm 0.03) < OSc_{,H2O2\text{-}NOx}$ (-0.21 ± 0.03) consistent with the oxidation conditions. The comparison between H_2O_2 only and H_2O_2-NO_X agrees with the finding that NO could enhance ·OH concentration (Li et al., 2015) and therefore enhance the overall extent of oxidation. Insignificant time evolution of H/C and O/C is observed for SOA formation from DEGEE (Fig. 6). The average H/C and O/C from precursors to SOA formed under different conditions are connected by the blue line in Fig. 6 to explore the major functionalization route associated with SOA formation under different conditions. It is noted that SOA formation under NO_X-only conditions is associated with a large change in H/C with only a slight change in O/C from precursor, indicating the importance of cyclization H loss (Fig. 6). A significant O/C increase with insignificant H/C decrease in SOA formed in presence of H_2O_2 relative to SOA formed under NO_X-only condition. This suggests carbonyl formation (hydrogen loss and oxygen gain) is more important during the oxidation of ether under H_2O_2-only than NO_X-only. SOA formed under NO-H_2O_2 condition leads to higher H/C and O/C than that under H_2O_2-only conditions indicating higher fraction of fragmentation pathway occurred than under H_2O_2-only conditions. This suggests that the presence of NO and further oxidation could lead to more volatile products during the oxidation of ether. The SOA difference (insignificant) in $f_{CO2}{}^+$ vs $f_{C2H3O}{}^+$ (Fig. S4) during ether oxidation under three different conditions agrees with the oxidation trend inferred from the elemental ratio trend.

The differences among SOA composition are further explored by comparing the representative peaks in the mass spectrum of HR-TOF-AMS (Table 2). Lower fraction of m/z 73 is observed in SOA formed in presence of H_2O_2-only than that under NO_X-only condition. This suggests that the cyclization is less important to SOA formation in presence of H_2O_2 when the level of oxidation is higher than that under the NO_X-only condition. This agrees with Section 3.4 that NO may lead to more

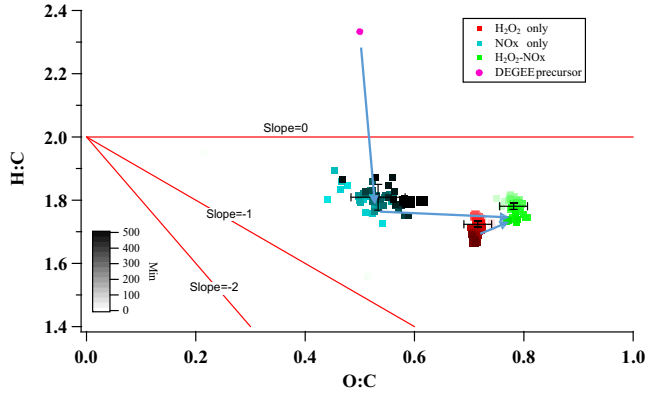

Fig. 6. H/C vs O/C of SOA formed from DEGEE under different reactivity (experimental data is colored proportional to the time of photooxidation from light to dark; the cross marked the average SOA elemental ratio location with standard deviation when significant particles are formed ($> 2\,\mu g\,m^{-3}$)); red lines represent the slope of different functionalization: alcohol/peroxide (slope = 0), carboxylic acid or alcohol + carbonyl on different carbons (slope = −1) and ketone/aldehyde (slope = −2) (Ng et al., 2011); blue lines connect the average (H/C, O/C) from precursor to the NOx only run, to the H_2O_2 only run and then to H_2O_2-NOx run. The error bars represent one standard deviation of H/C and O/C during the photooxidation of each experiment. H_2O_2 only: EPA1991A 40 ppb DEGEE + 1 ppm H_2O_2; NO only: EPA1993A 40 ppb DEGEE + 20 ppb NOx; H_2O_2-NO_X: EPA2059A 80 ppb DEGEE + 20 ppb NOx + 1 ppm H_2O_2. (For interpretation of the references to color in this figure legend, the reader is referred to the Web version of this article.)

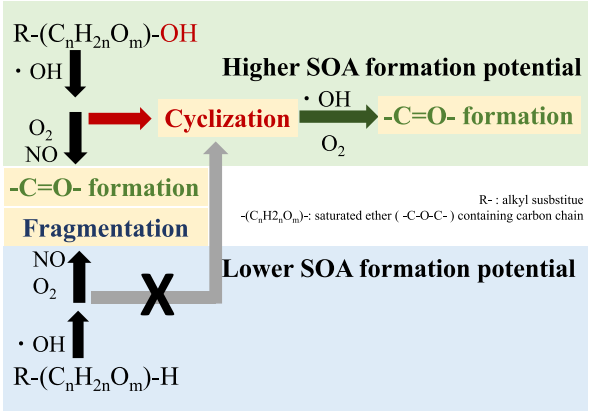

Fig. 7. General mechanism of ether photooxidation with and without –OH functional group in ethers.

fragmentation and thereby increases the importance of cyclic compounds to SOA formation. Insignificant m/z 61(carbonyl fragment) and a small fraction of m/z 87(carbonyl fragment) are found in SOA formed in the absence of H_2O_2 (NO_X-only). This confirms that carbonyl formation is less favored under lower levels of oxidation. It is also found the SOA formed in presence of NO and H_2O_2 shows a combination of representative peaks under NO_X-only and H_2O_2-only condition. The extent of oxidation under H_2O_2-NO condition is expected to be higher than that under H_2O_2-only conditions. The higher fraction of m/z 73 in SOA formed under H_2O_2-NO condition than that under H_2O_2 condition suggests that the contribution of cyclization to SOA formation dose not linearly decrease with the extent of oxidation.

4. Discussion

The formation of cyclic products during ether oxidation is proposed in this work (Fig. S5). Cyclic products reduce the C–C and C–O cleavage during oxidation reducing fragmentation and thereby lowers the overall volatility of the products. This work demonstrates that cyclization in ethers is determined by the presence of $–CH_2–O–CH_2CH_2OH$ in ether precursor. The cyclization pathway is critically important to SOA formation when fragmentation is promoted by NO. This suggests that forming cyclic products is important to SOA formation from ether under high NO_X urban area. Therefore, the contribution of ethers with $–CH_2–O–CH_2CH_2OH$ to atmospheric SOA formation is much more important than that without $–CH_2–O–CH_2CH_2OH$.

The assumption in this work that oxidized products have the same number of carbons (use of *O/M* and *Δ(H/M)* as their precursor is not perfect due to possible fragmentation and/or oligomerization that occurs during the oxidation process). However, use of *O/M* and *Δ(H/M)*) minimizes the discrepancy in elemental ratio resulting from the difference in oxygen to aliphatic carbon in the ether precursor. Therefore, analyzing SOA chemical composition on a precursor carbon number normalized basis (*O/M* and *-Δ(H/M)*) instead of a mole basis provides insight to the oxidation potential of different compounds and the role of different functional group in SOA formation. The finding that *O/M* is approximately 4 in SOA formed from ethers studied is similar to the observation that O/R is ~4 in SOA formed from aromatic hydrocarbons (Li et al., 2016a). The similarity in the oxidation of precursors to form SOA is likely to exist in other group of precursor species with similar functional groups. The method used therefore relates the SOA chemical composition with precursor molecular structure. It is valuable to apply the precursor structure based elemental ratio analysis method into the investigation of SOA formation from other groups of VOCs.

Summarily, the molecular structure is important to SOA formation from the photooxidation of ethers. The presence and location of –OH structure in ether determine SOA formation from ethers (Fig. 7). Cyclic products are formed in gas and particle phase during when an –OH group is present in an ether. The structure, $–CH_2–O–CH_2CH_2OH$, allows the glycol ether to cyclize such that the oxidation product remains at a sufficiently low volatility for SOA formation to occur in presence of NO_X. Further oxidation of glycol ethers lowers SOA yields by producing more fragmental products.

5. Atmospheric implication

The oxidation of ether is a combination of carbonyl formation, cyclization and fragmentation. Similar oxidation mechanisms are demonstrated among those ethers forming significant amounts of SOA. The molecular structures of ethers determine the branching ratio among carbonyl formation, cyclization and fragmentation. Cyclization is found to be an important mechanism during the oxidation of ethers and become critical to SOA formation when the oxidation level is more comparable to ambient. Cyclization is affected by the presence and location of –OH in the carbon bond of ethers and $–CH_2–O–CH_2CH_2OH$ structure is found to readily form cyclization products. Therefore, we consider DEGEE and DEGBE as two potentially important ethers that can contribute to SOA formation under atmospheric conditions. The total emissions from DEGBE and DEGEE are estimated as 2.04 TPD and 1.23 TPD in 2020, respectively (Cocker et al., 2014). SOA formation from the two glycol ethers in 2020 can then be estimated as 0.215 TPD in California State by assuming ambient organic concentration of $\sim 10\,\mu g{\cdot}m^{-3}$ (Jimenez et al., 2009) and predicting SOA yield based on two product model of DEGEE + NO (0.066). Mobile sources contribute to 85.3 TPD $PM_{2.5}$ in California (California Air Resource Board) and thereby approximately 25.6 TPD assuming organic aerosol accounts for 30% of $PM_{2.5}$ (Jimenez et al., 2009). Therefore, the contribution of glycol ethers to anthropogenic SOA is roughly 1% of the organic aerosol from mobile sources. Lower SOA formation from mobile sources due to tightening emission standards while higher emissions from consumer products are expected based on current regulations. Therefore, glycol ethers used in consumer products might play an important role in anthropogenic SOA formation in the near future.

Acknowledgment

We acknowledge funding support from California Air Resource Board (13-302) and W. M. Keck Foundation. Any opinions, findings, and conclusions expressed in this material are those of the author(s) and do not necessarily reflect the views of the CARB.

Appendix A. Supplementary data

Supplementary data related to this article can be found at http://dx.doi.org/10.1016/j.atmosenv.2017.12.025.

References

Aiken, A.C., DeCarlo, P.F., Jimenez, J.L., 2007. Elemental analysis of organic species with electron ionization high-resolution mass spectrometry. Anal. Chem. 79 (21), 8350–8358.

Aiken, A.C., DeCarlo, P.F., Kroll, J.H., Worsnop, D.R., Huffman, J.A., Docherty, K.S., Ulbrich, I.M., Mohr, C., Kimmel, J.R., Sueper, D., Sun, Y., Zhang, Q., Trimborn, A., Northway, M., Ziemann, P.J., Canagaratna, M.R., Onasch, T.B., Alfarra, M.R., Prevot, A.S.H., Dommen, J., Duplissy, J., Metzger, A., Baltensperger, U., Jimenez, J.H., 2008. O/C and OM/OC ratios of primary, secondary, and ambient organic aerosols with high-resolution time-of-flight aerosol mass spectrometry. Environ. Sci. Technol. 42 (12), 4478–4485.

Aschmann, S.M., Atkinson, R., 1998. Kinetics of the gas-phase reactions of the OH radical with selected glycol ethers, glycols, and alcohols. Int. J. Chem. Kinet. 30, 533–540.

Aschmann, S.M., Atkinson, R., 1999. Products of the gas-phase reactions of the OH radical with n-butyl methyl ether and 2-isopropoxyethanol: reactions of ROC(O) < radicals. Int. J. Chem. Kinet. 31, 501–513. http://dx.doi.org/10.1002/(sici)1097-4601(1999)31:7<501::aid-kin5>3.0.co;2-h.

Canagaratna, M.R., Jayne, J.T., Jimenez, J.L., Allan, J.D., Alfarra, M.R., Zhang, Q., Onasch, T.B., Drewnick, F., Coe, H., Middlebrook, A., Delia, A., Williams, L.R., Trimborn, A.M., Northway, M.J., DeCarlo, P.F., Kolb, C.E., Davidovits, P., Worsnop, D.R., 2007. Chemical and microphysical characterization of ambient aerosols with the aerodyne aerosol mass spectrometer. Mass Spectrom. Rev. 26 (2), 185–222.

California Air Resource Board, Almanac Emission Projection Data 2012 Estimated Annual Average Emissions, http://www.arb.ca.gov/app/emsinv/2013/emseic1_query.php?F_DIV=-4&F_YR=2012&F_SEASON=A&SP=2013&F_AREA=CA.

Carter, W.P.L., Cocker III, D.R., Fitz, D.R., Malkina, I.L., Bumiller, K., Sauer, C.G., Pisano, J.T., Bufalino, C., Song, C., 2005. A new environmental chamber for evaluation of gas-phase chemical mechanisms and secondary aerosol formation. Atmos. Environ. 39, 7768–7788. http://dx.doi.org/10.1016/j.atmosenv.2005.08.040.

Chew, A.A., Atkinson, R., Aschmann, S.M., 1998. Kinetics of the gas-phase reactions of NO_3 radicals with a series of alcohols, glycol ethers, ethers and chloroalkenes. J. Chem. Soc. Faraday T. 94, 1083–1089.

Chhabra, P.S., Ng, N.L., Canagaratna, M.R., Corrigan, A.L., Russell, L.M., Worsnop, D.R., Flagan, R.C., Seinfeld, J.H., 2011. Elemental composition and oxidation of chamber organic aerosol. Atmos. Chem. Phys. 11 (17), 8827–8845.

Choi, H., Schmidbauer, N., Spengler, J., Bornehag, C.-G., 2010. Sources of propylene glycol and glycol ethers in air at home. Int. J. Environ. Res. Publ. Health 7, 4213–4237.

Collins, E., Sidebottom, H.W., Wenger, J.C., Calvé, S.L., Mellouki, A., LeBras, G., Villenave, E., Wirtz, K., 2005. The influence of reaction conditions on the photo-oxidation of diisopropyl ether. J. Photochem. Photobiol., A 176, 86–97.

Cooper, S.D., Raymer, J.H., Pellizzari, E., Thomas, K.W., 1995. The identification of polar organic compounds found in consumer products and their toxicological properties. J. Expo. Anal. Environ. Epidemiol. 5, 57–75.

Cocker III, D.R., Li, L., Price, J.D., Kacarab, M., Chen, C.-L., 2014. Review of VOC Emissions Inventory for Consumer Products and Architectural Coatings for Potential Alternative Fate and Availability Corrections. Consumer Specialty Products Association Report. .

DeCarlo, P.F., Kimmel, J.R., Trimborn, A., Northway, M.J., Jayne, J.T., Aiken, A.C., Gonin, M., Fuhrer, K., Horvath, T., Docherty, K.S., Worsnop, D.R., Jimenez, J.L., 2006. Field-deployable, high-resolution, time-of-flight aerosol mass spectrometer. Anal. Chem. 78 (24), 8281–8289.

Donahue, N.M., Kroll, J., Pandis, S.N., Robinson, A.L., 2012. A two-dimensional volatility basis set–Part 2: diagnostics of organic-aerosol evolution. Atmos. Chem. Phys. 12 (2), 615–634.

Eberhard, J., MüLler, C., Stocker, D.W., Kerr, J.A., 1993. The photo-oxidation of diethyl ether in smog chamber experiments simulating tropospheric conditions: product studies and proposed mechanism. Int. J. Chem. Kinet. 25, 639–649.

Environmental Protection Agency United States, 2000. Toxics Release Inventory-list of Toxic Chemicals within the Glycol Ethers Category.

Espada, C., Shepson, P.B., 2005. The production of organic nitrates from atmospheric oxidation of ethers and glycol ethers. Int. J. Chem. Kinet. 37, 686–699.

Fromme, H., Nitschke, L., Boehmer, S., Kiranoglu, M., Göen, T., 2013. Exposure of German residents to ethylene and propylene glycol ethers in general and after cleaning scenarios. Chemosphere 90, 2714–2721.

Geiger, H., Becker, K., 1999. Degradation mechanisms of dimethoxymethane and dimethoxyethane in the presence of NOx. Atmos. Environ. 33, 2883–2891.

Gibson, W., Keller, P., Foltz, D., Harvey, G., 1991. Diethylene glycol mono butyl ether concentrations in room air from application of cleaner formulations to hard surfaces. J. Expo. Anal. Environ. Epidemiol. 1, 369–383.

Hall, W.A., Pennington, M.R., Johnston, M.V., 2013. Molecular transformations accompanying the aging of laboratory secondary organic aerosol. Environ. Sci. Technol. 47 (5), 2230–2237.

Heald, C.L., Kroll, J.H., Jimenez, J.L., Docherty, K.S., DeCarlo, P.F., Aiken, A.C., Chen, Q., Martin, S.T., Farmer, D.K., Artaxo, P., 2010. A simplified description of the evolution of organic aerosol composition in the atmosphere. Geophys. Res. Lett. 37 (8).

Jenkin, M.E., Hayman, G.D., Wallington, T.J., Hurley, M.D., Ball, J.C., Nielsen, O.J., Ellermann, T., 1993. Kinetic and mechanistic study of the self-reaction of methoxymethylperoxy radicals at room temperature. J. Phys. Chem. 97, 11712–11723.

Jimenez, J.L., Canagaratna, M.R., Donahue, N.M., Prevot, A.S.H., Zhang, Q., Kroll, J.H., DeCarlo, P.F., Allan, J.D., Coe, H., Ng, N.L., Aiken, A.C., Docherty, K.S., Ulbrich, I.M., Grieshop, A.P., Robinson, A.L., Duplissy, J., Smith, J.D., Wilson, K.R., Lanz, V.A., Hueglin, C., Sun, Y.L., Tian, J., Laaksonen, A., Raatikainen, T., Rautiainen, J., Vaattovaara, P., Ehn, M., Kulmala, M., Tomlinson, J.M., Collins, D.R., Cubison, M.J., Dunlea1, E.,J., Huffman, J.A., Onasch, T.B., Alfarra, M.R., Williams, P.I., Bower, K., Kondo, Y., Schneider, J., Drewnick, F., Borrmann, S., Weimer, S., Demerjian, K., Salcedo, D., Cottrell, L., Griffin, R., Takami, A., Miyoshi, T., Hatakeyama, S., Shimono, A., Sun, J.Y., Zhang, Y.M., Dzepina, K., Kimmel, J.R., Sueper, D., J. Jayne, T., Herndon, S.C., Trimborn, A.M., Williams, L.R., Wood, E.C., Middlebrook, A.M., Kolb, C.E., Baltensperger, U., Worsnop, D.R., 2009. Evolution of organic aerosols in the atmosphere. Science 326 (5959), 1525–1529.

Johnson, D., Andino, J.M., 2001. Laboratory studies of the ·OH-initiated photooxidation of ethyl-n-butyl ether and di-n-butyl ether. Int. J. Chem. Kinet. 33, 328–341.

Kroll, J.H., Donahue, N.M., Jimenez, J.L., Kessler, S.H., Canagaratna, M.R., Wilson, K.R., Altieri, K.E., Mazzoleni, L.R., Wozniak, A.S., Bluhm, H., Mysak, E.R., Smith, J.D., Kolb, C.E., Worsnop, D., 2011. R.: carbon oxidation state as a metric for describing the chemistry of atmospheric organic aerosol. Nat. Chem. 3 (2), 133–139.

Li, L., Tang, P., Cocker III, D.R., 2015. Instantaneous nitric oxide effect on secondary organic aerosol formation from *m*-xylene photooxidation. Atmos. Environ. 119, 144–155.

Li, L., Tang, P., Nakao, S., Kacarab, M., Cocker III, D.R., 2016a. Novel approach for evaluating secondary organic aerosol from aromatic hydrocarbons: unified method for predicting aerosol composition and formation. Environ. Sci. Technol. 50 (12), 6249–6256.

Li, L., Tang, P., Nakao, S., Chen, C.-L., Cocker III, D.R., 2016b. Role of methyl group number on SOA formation from monocyclic aromatic hydrocarbons photooxidation under low-NOx conditions. Atmos. Chem. Phys. 16 (4), 2255–2272.

Malanca, F.E., Fraire, J.C., Argüello, G.A., 2009. Kinetics and reaction mechanism in the oxidation of ethyl formate in the presence of NO_2: atmospheric implications. J. Photochem. Photobiol., A 204, 75–81.

McLafferty, F.W., Tureček, F., 1993. Interpretation of Mass Spectra. Univ Science Books.

Mellouki, A., Teton, S., Le Bras, G., 1995. Kinetics of OH radical reactions with a series of ethers. Int. J. Chem. Kinet. 27, 791–805.

Mellouki, A., Le Bras, G., Sidebottom, H., 2003. Kinetics and mechanisms of the oxidation of oxygenated organic compounds in the gas phase. Chem. Rev. 103, 5077–5096.

Nazaroff, W.W., Weschler, C.J., 2004. Cleaning products and air fresheners: exposure to primary and secondary air pollutants. Atmos. Environ. 38, 2841–2865.

Ng, N., Canagaratna, M., Jimenez, J., Chhabra, P., Seinfeld, J., Worsnop, D., 2011. Changes in organic aerosol composition with aging inferred from aerosol mass spectra. Atmos. Chem. Phys. 11, 6465–6474.

Odum, J.R., Hoffmann, T., Bowman, F., Collins, D., Flagan, R.C., Seinfeld, J.H., 1996. Gas/particle partitioning and secondary organic aerosol yields. Environ. Sci. Technol. 30, 2580–2585.

Orlando, J.J., 2007. The atmospheric oxidation of diethyl ether: chemistry of the C_2H_5–O–CH (O˙) CH_3 radical between 218 and 335 K. Phys. Chem. Chem. Phys. 9, 4189–4199.

Pankow, J.F., Asher, W.E., 2008. SIMPOL. 1: a simple group contribution method for predicting vapor pressures and enthalpies of vaporization of multifunctional organic compounds. Atmos. Chem. Phys. 8, 2773–2796.

Platz, J., Sehested, J., Nielsen, O., Wallington, T., 1999. Atmospheric chemistry of trimethoxymethane, $(CH_3O)_3CH$; Laboratory studies. J. Phys. Chem. A. 103, 2632–2640.

Porter, E., Wenger, J., Treacy, J., Sidebottom, H., Mellouki, A., Téton, S., LeBras, G., 1997. Kinetic studies on the reactions of hydroxyl radicals with diethers and hydroxyethers. J. Phys. Chem. A. 101, 5770–5775.

Pye, H.O., Seinfeld, J.H., 2010. A global perspective on aerosol from low-volatility organic compounds. Atmos. Chem. Phys. 10, 4377–4401.

Sehested, J., Møgelberg, T., Wallington, T., Kaiser, E., Nielsen, O., 1996. Dimethyl ether oxidation: kinetics and mechanism of the $CH_3OCH_2 + O_2$ reaction at 296 K and 0.38-940 torr total pressure. J. Phys. Chem. 100, 17218–17225.

Singer, B.C., Destaillats, H., Hodgson, A.T., Nazaroff, W.W., 2006. Cleaning products and air fresheners: emissions and resulting concentrations of glycol ethers and terpenoids. Indoor Air 16, 179–191.

Španěl, P., Ji, Y., Smith, D., 1997. SIFT studies of the reactions of H_3O^+, NO^+ and O_2^+ with a series of aldehydes and ketones. Int. J. Mass Spectrom. 165, 25–37.

Stemmler, K., Mengon, W., Kerr, J.A., 1996. OH radical initiated photooxidation of 2-ethoxyethanol under laboratory conditions related to the troposphere: product studies and proposed mechanism. Environ. Sci. Technol. 30, 3385–3391.

Tommaso, S.D., Rotureau, P., Crescenzi, O., Adamo, C., 2011. Oxidation mechanism of diethyl ether: a complex process for a simple molecule. Phys. Chem. Chem. Phys. 13, 14636–14645.

Tuazon, E.C., Carter, W.P., Aschmann, S.M., Atkinson, R., 1991. Products of the gas-phase reaction of methyl tert-butyl ether with the OH radical in the presence of NOx. Int. J. Chem. Kinet. 23, 1003–1015.

Tuazon, E.C., Aschmann, S.M., Atkinson, R., 1998. Products of the gas-phase reactions of the OH radical with 1-methoxy-2-propanol and 2-butoxyethanol. Environ. Sci. Technol. 32, 3336–3345.
Võ, U.-U.T., Morris, M.P., 2014. Nonvolatile, semivolatile, or volatile: redefining volatile for volatile organic compounds. J. Air. Waste. Manage. Assoc. 64, 661–669.
Wallington, T.J., Japar, S.M., 1991. Atmospheric chemistry of diethyl ether and ethyl tert-butyl ether. Environ. Sci. Technol. 25, 410–415.
Wenger, J., Porter, E., Collins, E., Treacy, J., Sidebottom, H., 1999. Mechanisms for the chlorine atom initiated oxidation of dimethoxymethane and 1, 2-dimethoxyethane in the presence of NO_X. Chemosphere 38, 1197–1204.
Wieslander, G., Norbäck, D., 2010a. A field study on clinical signs and symptoms in cleaners at floor Polish removal and application in a Swedish hospital. Int. Arch. Occ. Env. Hea. 83, 585–591.
Wieslander, G., Norbäck, D., 2010b. Ocular symptoms, tear film stability, nasal patency, and biomarkers in nasal lavage in indoor painters in relation to emissions from water-based paint. Int. Arch. Occ. Env. Hea. 83, 733–741.
Zhu, J., Cao, X.-L., Beauchamp, R., 2001. Determination of 2-butoxyethanol emissions from selected consumer products and its application in assessment of inhalation exposure associated with cleaning tasks. Environ. Int. 26, 589–597.